ESA CONTRACT REPORT

Contract Report to the European Space Agency

ECMWF Final Report on SMOS brightness temperature activities over land: Monitoring and Data Assimilation

Patricia de Rosnay, Joaquín Muñoz Sabater, Clément Albergel, Heather Lawrence, Lars Isaksen and Steve English

ESA Technical Officer: M. Drusch

ESA/ESRIN Contract 4000101703/10/NL/FF/fk

European Centre for Medium-Range Weather Forecasts
Europäisches Zentrum für mittelfristige Wettervorhersage
Centre européen pour les prévisions météorologiques à moyen terme

ECMWF

Series: ECMWF ESA Project Report Series

A full list of ECMWF Publications can be found on our web site under:
http://www.ecmwf.int/en/research/publications

Contact: library@ecmwf.int

European Centre for Medium Range Weather Forecasts
Shinfield Park, Reading, RG2 9AX, England

Contract Report to the European Space Agency

ECMWF Final Report on SMOS brightness temperature activities over land: Monitoring and Data Assimilation

Authors: Patricia de Rosnay, Joaquín Muñoz Sabater, Clément Albergel, Heather Lawrence, Lars Isaksen and Steve English

ESA Technical Officer: M. Drusch
ESA/ESRIN Contract 4000101703/10/NL/FF/fk

European Centre for Medium-Range Weather Forecasts
Shinfield Park, Reading, Berkshire, UK

1 March 2019

	Name	Company
First version prepared by (September 2016)		ECMWF
Quality Visa		ECMWF
Application Authorised by		ESA/ESRIN

Distribution list:

ESA/ESRIN
Susanne Mecklenburg
ESA ESRIN Documentation Desk

ESA/ESTEC
Matthias Drusch

ECMWF
Stephen English

Executive Summary

This paper is the final report of the SMOS project activities conducted at ECMWF between 2007 and 2018 to use SMOS brightness temperature (TB) observations in the ECMWF Integrated Forecasting System (IFS) for monitoring and data assimilation purposes. These activities were conducted in two phases. The first one, (contract 20244/07/I-LG) focused on the implementation of the SMOS TB data in the IFS and the development of the SMOS TB monitoring system. It included the development of the SMOS forward model CMEM (the Community Microwave Emission Modelling platform) as well as a number of technical tasks such as the SMOS BUFR specification, the SMOS Observation Data Base, and the set-up of the SMOS monitoring pages. The second phase (contract No 4000101703/10/NL/FF/fk) was dedicated to SMOS TB data assimilation. It included the implementation of the SMOS TB data in the Simplified Extended Kalman Filter data assimilation system, further developments of the forward model CMEM, bias correction, long term monitoring, tuning and specification of the background and observation errors specification, and evaluation and SMOS TB data assimilation in the IFS. Activities conducted in 2016-2018 also included the SMOS neural network developments and offline data assimilation as well as ocean activities (sea ice and wind speed), which are reported separately and therefore not included in this paper. Both contracts included technical support activities like the definition of the SMOS DPGS interface and Interface Control Document (ICD) and support to ESA with ECMWF products and changes related to new IFS cycles, resolution and format changes. Long term monitoring results over land showed that SMOS and ECMWF reanalysis-based brightness temperature agreement steadily improved between 2010 and 2016, indicating improvement of SMOS products quality through the SMOS lifetime. Data assimilation results showed that the soil moisture state benefits from the direct assimilation of SMOS TB, especially in better representing the temporal variations of soil moisture in time. The forecasting skills of low level atmospheric variables remains mainly driven by the screen level observations. Despite the clear benefits on the soil state, remote sensing data needs to be used with screen level variables to add value on the state of the atmosphere, pointing to inconsistencies in the physical coupling between the land and near-surface components of the ECMWF Earth system. These activities demonstrated the relevance of the SMOS observations for numerical weather prediction modelling and assimilation developments.

Contents

1 Introduction

Satellite based soil moisture observations from space are of high interest for Numerical Weather Prediction (NWP) applications. They have the capability to provide in Near Real Time (NRT) consistent information across all continental surfaces. The Soil Moisture and Ocean Salinity (SMOS) mission, launched in November 2009, was designed for soil measurements from space purposes. It provides L-band (1.4 GHz) passive measurements which are optimal, both in terms of accuracy and sampling depth, for soil moisture remote sensing (Kerr et al., 2001). SMOS is the second Earth's Explorer mission of the European Space Agency (ESA) Living Planet Programme, exploring an innovative remote sensing technique based on radiometric aperture synthesis to observe soil moisture over continental surfaces and ocean salinity over oceans (Kerr et al., 2010; Mecklenburg et al., 2016).
Contracted by ESA, the European Centre for Medium-Range Weather Forecasts (ECMWF) has developed and implemented global monitoring and data assimilation of the Soil Moisture and Ocean Salinity (SMOS) mission data. In a first phase project (2007-2010), the ECMWF operational Integrated Forecasting System (IFS) was updated to acquire, process, and archive SMOS NRT brightness temperatures, and the NRT SMOS brightness temperature data monitoring was implemented. In NWP systems, monitoring is mainly focused on the comparison between the observed variable and the model equivalent simulating that observation, because this is the quantity used in the analysis. The Community Microwave Emission Modelling platform (CMEM) was developed for this purpose in the context of this contract. The resulting framework made it possible to obtain daily statistics of the observations, the model equivalent, and the difference between the two quantities (first-guess departures). In the second phase project (2010-2018), ECMWF developed SMOS brightness temperatures (TB) data assimilation in their land surface SEKF (Simplified Extended Kalman Filter). The main objectives were (1) to produce, validate, and disseminate a SMOS Level-3 root zone soil moisture product, and to exploit the SMOS NRT brightness temperatures, (2) to quantify the impact of the SMOS observations, and compare it to that of other soil moisture related observations, on the predictive skill of the forecasting system, and (3) to provide long term assessment of the SMOS data quality based on reanalysis based-long term monitoring.

This paper is the final report of the SMOS activities conducted at ECMWF between 2007 and 2018 for SMOS TB data monitoring and assimilation over land surfaces. Activities conducted in 2016-2018 also included the SMOS neural network developments and offline data assimilation as well as ocean activities (sea ice and wind speed), which are reported separately and therefore not included in this paper.

The contractual context of this work is presented in the next section, completed by an inventory provided in the appendix with all the reports, technical memorandum, newsletter articles, peer reviewed articles produced under this contract. Section 3 gives a summary of the main results of the SMOS activities conducted at ECMWF to use brightness temperature over land. It highlights the main outcomes of the research and operational implementations. Section 4 concludes.

2 Contractual context and deliverables

The first phase of the SMOS TB study over land was conducted at ECMWF from August 2007 to June 2010 (35 months) under the ESA/ESRIN Contract 20244/07/I-LG. The total funding provided to ECMWF by ESA corresponded to 27 person-month. Under this contract the operational Integrated Forecasting System (IFS) has been updated to acquire, process, and archive SMOS near real time (NRT) brightness temperatures. The work accomplished during this first phase comprised:

- The definition of the Level-1C Near-Real-Time product, SMOS BUFR specification (de Rosnay et al., 2012),

- The development and implementation of the Community Microwave Emission Model, MS1TN-P1 (de Rosnay et al., 2009b)
- The operational acquisition of SMOS data at ECMWF;
- The implementation of the SMOS data in the Integrated Forecasting System (IFS) through the SMOS Observation Data Base (ODB), MS1TN-P2 (Muñoz-Sabater et al., 2009)
- The test and validation of the acquisition and pre-processing of the SMOS data in the IFS, MS2TN-P1/2/3 (Muñoz-Sabater et al., 2010)
- The implementation of SMOS monitoring system (now at `https://www.ecmwf.int/en/forecasts/charts/obstat/?facets=Instrument,SMOS`) and provision of SMOS continuous monitoring report part1 (Muñoz-Sabater et al., 2011c).

The list of deliverables, including Milestone (MS) Technical Notes (TN), provided under this contract is given in the top part of Table 1. SMOS data was implemented in the IFS for the purpose of SMOS monitoring activities. SMOS data implementation in the IFS has been a challenging task due to the characteristics of this new type of data combined to its large volume. The amount of SMOS data had to be reduced by 90%, based on a random selection of the data (and also filters out non-physical brightness Temperatures values below 50K or above 350K). This data thinning approach has proved to be efficient enough to enable to put SMOS data in the ODB as the angular signature is maintained. It made it possible to use SMOS data in the IFS very soon after the first SMOS data was made available.

The second phase of the SMOS TB study at ECMWF was conducted from October 2010 to December 2018 (99 months) under the ESA/ESRIN contract 4000101703/10/NL/FF/fk. The total funding provided to ECMWF by ESA for land surface activities corresponded to 63 person-month, of which 50 person-month related to brightness temperature activities over land summarised in this report. The main objective of this phase was to focus on scientific analysis of SMOS monitoring results and investigations of the SMOS data assimilation impact on the forecasts skills. It included CMEM configuration, bias correction, the development of a flexible data thinning, noise filtering approach, implementation of the SMOS data in the SEKF soil analysis, sensitivity study of the SMOS Jacobians, tuning of the observation and background error specifications and evaluation of the data assimilation impact for different configuration of the observing system, using SMOS TB data with and without other sources of information used in NWP land analysis systems such as the ASCAT soil moisture product and the screen level observations. This second phase followed a progressive approach structured with several Contract Change Notices (CCN).

- Main contract (28 peron-month), following the Request for Clarification (RfQ) 3/13053/09/NL/FF/FK, to focus on SMOS NRT processing Muñoz-Sabater et al. (2011a), bias correction de Rosnay et al. (2018), implementation of SMOS data in the SEKF Muñoz-Sabater and de Rosnay (2011); Muñoz-Sabater et al. (2011d), data assimilation tests and production of a SMOS Level-3 root zone soil moisture Muñoz-Sabater et al. (2014a, 2013).
- CCN1 (14 person-month) from November 2012 to December 2013, CCN2 (January 2014 to February 2014) and CCN3 (March 2014 to 15 September 2014) supported operational monitoring activities, root zone soil moisture activities and configuration of the data assimilation system Muñoz-Sabater (2015); Muñoz-Sabater et al. (2018), with in particular a study of the error matrices structure Muñoz-Sabater et al. (2016a).
- CCN4 from 16 September 2014 to 15 March 2016, and CCN5 from 16 March 2016 to 15 June 2016, started to look at SMOS phase III activities: Toward ocean applications. This CCNs represented 8 person-month for ESA support and a comprehensive SMOS TB data assimilation study Muñoz-Sabater et al.

Phase I, Contract 20244/07/I-LG, August 2007 - June 2010		
MS1TN-Part 1	de Rosnay et al. (2009b)	Global Surface Emission model
MS1TN-Part 2	Muñoz-Sabater et al. (2009)	IFS interface
MS2TN-Part 1/2/3	Muñoz-Sabater et al. (2010)	Operational Pre-processing chain, Collocation software development and Offline monitoring suite
Monitoring Report	Muñoz-Sabater et al. (2011c)	SMOS continuous monitoring report part1
Phase II, Contract 4000101703/10/NL/FF/fk, October 2010 - December 2018		
Monitoring webpage	https://www.ecmwf.int/en/forecasts/charts/obstat/?facets=Instrument,SMOS	
TN-PII-WP1100	Muñoz-Sabater et al. (2011a)	SMOS Monitoring Report Number 2
TN-PII-WP1300	Muñoz-Sabater and de Rosnay (2011)	SMOS Report on noise filtering
TN-PII-WP1200	Muñoz-Sabater et al. (2011d)	SMOS Report on data thinning
TN-PII-WP2000-2100	Muñoz-Sabater et al. (2014a)	Report on Level 3 root zone soil moisture and DA Impact
TN-PII-WP2300	Muñoz-Sabater et al. (2013)	Hot Spot Analysis
TN-PII-WP3401-3402	Muñoz-Sabater et al. (2016a)	SMOS Report on background and observation error scenarios
TR2PIII-WP4020	Muñoz-Sabater et al. (2016b)	SMOS Near-Real-Time Soil Moisture processor: Operational chain and evaluation
TR4PIII-WP4050	Tietsche and Balmaseda (2016)	Sea-ice thickness from SMOS
TR5PIII-WP4060	De Chiara and English (2016)	SMOS Hurricane wind speed analysis
TR1PIII-WP4010	Rodríguez-Fernández et al. (2017a)	SMOS Neural Network Soil Moisture Data Assimilation
MS3TN-Part2	de Rosnay et al. (2018)	SMOS brightness temperature forward modelling, bias correction and long term monitoring at ECMWF
TR3PIII-WP4040	Muñoz-Sabater et al. (2019)	Assimilation of SMOS brightness temperature in the ECMWF Integrated Forecasting System
Final Report	This report de Rosnay et al. (2019b)	Final Report on SMOS brightness temperature activities over land: Monitoring and Data Assimilation
Technical tasks to support to the ESA SMOS mission		
Level-1C NRT product	BUFR Specification (de Rosnay et al., 2012)	
SMOS DPGS interface	ICD document (Flati et al., 2013)	
SMOS QWG	Contribution and participation to the SMOS QWG	
IFS dissemination	Continuous support to ESA with new IFS cycles products	

Table 1: SMOS ECMWF delivered reports during the first phase contract 2007-2010 and the second phase contract 2010-2018, and support tasks. Reports in the shaded grey lines are on ocean and neural network activities which are not summarised in this final report.

(2019); de Rosnay et al. (2019a). It also included 13 person-month for other land activities for SMOS Neural Network (NN) implementation for ESA Muñoz-Sabater et al. (2016b); Rodríguez-Fernández et al. (2016, 2017b) and SMOS NN offline assimilation Rodríguez-Fernández et al. (2017a), and 9 person-month for ocean sea ice and wind activities Tietsche and Balmaseda (2016); De Chiara and English (2016) not reported here.

- CCN6 (01 June 2016 - 31 December 2018) focused on SMOS ocean activities (not reported here).

The list of deliverables of the Phase II of the contract is given in Table 1. The list of reports, technical memorandum, newsletter articles, peer reviewed articles produced during the two phases of the contract is given at the end of the paper as an appendix. As indicated above, this Final Report gives an overview of the SMOS TB activities conducted over land. SMOS neural network activities and SMOS ocean activities are reported separately.

Results allowed defining the best data assimilation system configuration in the current IFS to use for future data assimilation experiments. They showed that the combined effect of doubling the error of the SMOS observations and a B matrix as a function of soil texture are expected to produce best results both, in terms of lower RMSD and higher R with in-situ data. In terms of atmospheric impact, combining the SMOS brightness temperature observations with screen level observations in the data assimilation system was shown to provide the best results in terms of combined impact on soil moisture and atmospheric forecasts. These findings were used to define the set-up of SMOS brightness temperature data assimilation experiments.

Beside the provision of deliverables directly related to the contract, a number of continuous tasks were conducted to support the SMOS mission and ESA SMOS activities (Table 1, bottom). These activities include regular interactions with ESA regarding the SMOS BUFR specification, the definition and maintenance of the SMOS DPGS interface and Interface Control Document (ICD), the maintenance of the SMOS monitoring pages, contribution and participation to the SMOS Quality Working Group (QWG), and support to ESA regarding new IFS cycles implementation and provision of test (e-suite) sets of files.

3 Results and highlights

3.1 SMOS global surface emission model

The SMOS activities started at ECMWF in 2007 with the development of the Community Microwave Emission Model (CMEM). CMEM was later renamed (during the second phase of the project) to become the Community Microwave Emission Modelling platform which refers to its modular and multi-parameterisation specificities. CMEM was developed to be used as the forward operator for low frequency passive microwave brightness temperatures (from 1GHz to 20 GHz) of the surface. CMEM's physics is based on the parameterisations used in the L-Band Microwave Emission of the Biosphere and Land Surface Microwave Emission Model. CMEM modularity allows considering different parameterisations of the soil dielectric constant as well as different soil approaches and effective temperature, roughness, vegetation and atmospheric contribution opacity models.
Figure 1 shows the CMEM code structure as developed during the first phase of the contract and as implemented in the IFS. Figure 1 also illustrates results obtained with CMEM at C-band for different precipitation forcing with the land surface model ORCHIDEE, compared to AMSR-E observations over West Africa in summer 2006 de Rosnay et al. (2009a). L-band observations from the SMOSREX (Soil Monitoring Of the Soil Reservoir EXperiment) field experiment were also used to calibrate the soil roughness parameterisations of CMEM as described in Muñoz-Sabater et al. (2011b). Furthermore, the Skylab observation were used to compare CMEM's parameterisations using the few orbit swaths available providing space-based L-band observations Drusch et al. (2009a).

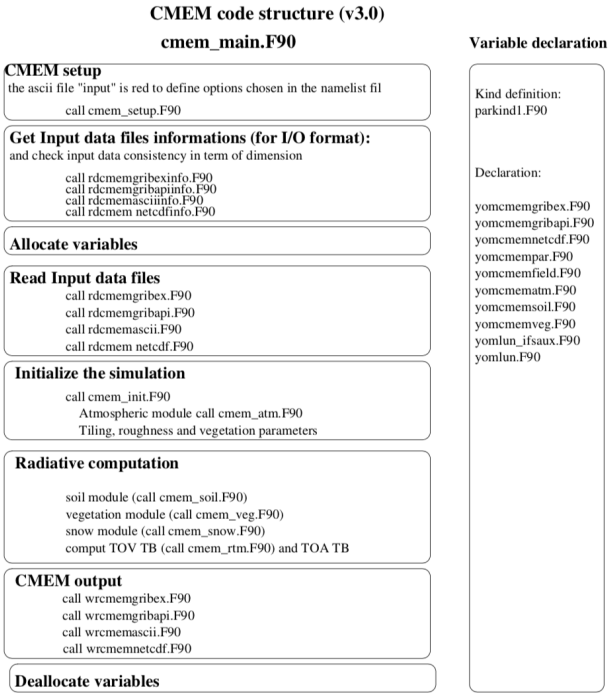

(a) CMEM code structure

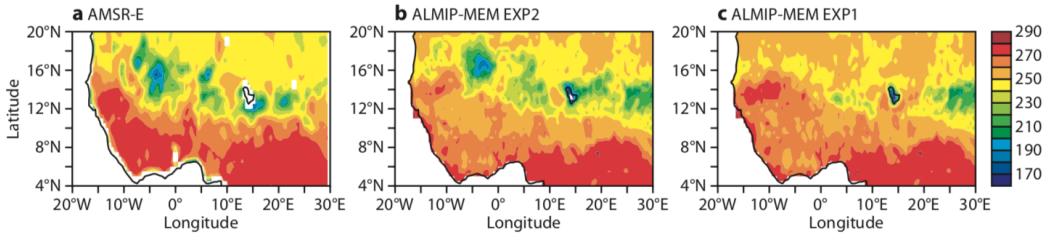

(b) C-band observations and CMEM simulations on 20-21 July 2006

Figure 1: Top panel: CMEM code structure as available at the end of the first phase of the project. Bottom panel: C-band brightness temperature at horizontal polarisation on 20-21 July 2006 observed by AMSR-E (left), simulations in ALMIP-MEM for different precipitation forcing (middle and right panel). Figure from MS1TN-Part 1 (de Rosnay et al., 2009b).

.

CMEM was released on the ECMWF web site under tagged versions from December 2007 onwards and it has been used by a number of users for SMOS and SMAP applications, such as for example studies from Carrera et al. (2015) or Lievens et al. (2015), benefiting the NWP and hydrological communities. Further developments of CMEM, mainly related to the optimisation of CMEM's configuration using SMOS observations, were conducted in the second phase of the project as summarised in Section 3.10.

The development of CMEM was largely supported by this project before the SMOS launch and led to a dedicated report delivered in the project Phase I (MS1TN-Part1, see Table 1) by de Rosnay et al. (2009b) and a number of related publications (Holmes et al., 2008; Drusch et al., 2009a; de Rosnay et al., 2009a; Muñoz-Sabater et al., 2011b).

3.2 IFS interface

The technical implementation of the SMOS data in the Integrated Forecast System (IFS) started before the SMOS launch using simulated Level 1 NRT test data provided by ESA. The SMOS NRT products are processed at the European Space Astronomy Centre (ESAC) in Madrid (Spain) and sent to ECMWF via the SMOS Data Processing Ground Segment (DPGS) interface. The product used at ECMWF is the NRT product which are geographically sorted swath-based maps of brightness temperatures. The geolocated product received at ECMWF is provided on an equal area grid system called ISEA 4H9 (Icosahedron Snyder Equal Area grid with Aperture 4 at resolution 9). A significant activity during the SMOS project at ECMWF was to implement the SMOS data at ECMWF, with the main objective being to be ready for SMOS monitoring as soon as possible after the launch. The main steps to achieve this were:

- To put in place an operational acquisition of the SMOS data at ECMWF, and archive the data on ECMWF's File Storage system (ECFS),
- Conversion of NRT test Binary Universal Form for the Representation of meteorological data (BUFR) product to internal ECMWF BUFR format,
- Pre-screening of BUFR data (preliminary thinning and consistency checks),
- Conversion of SMOS BUFR data to the ECMWF Observational Data Base (ODB) format for use in the IFS,
- Computations in model space of observations with model fields.

The technical implementation is illustrated in Figure 2 which shows the dedicated SMOS tasks in the IFS observation family on the left, and preliminary maps of SMOS TB in the ODB obtained using simulated Level 1 NRT test data provided by ESA before the SMOS launch. The detailed documentation of the IFS interface with SMOS data is provided in the report (MS1TN-P2, see Table 1) delivered by Muñoz-Sabater et al. (2009).

3.3 Operational Pre-processing chain, Collocation software development and Offline monitoring suite

Further to the IFS interface developments, quality checks were implemented both in the ECMWF acquisition and in the IFS. These included generic checks on the SMOS data file format (e.g. checks on the BUFR headers, date and time, and structure), as well as preliminary data quality check in the pre-processing to ensure that brightness temperatures are in the range of physically reasonable values, concretely not lower than 50 K and

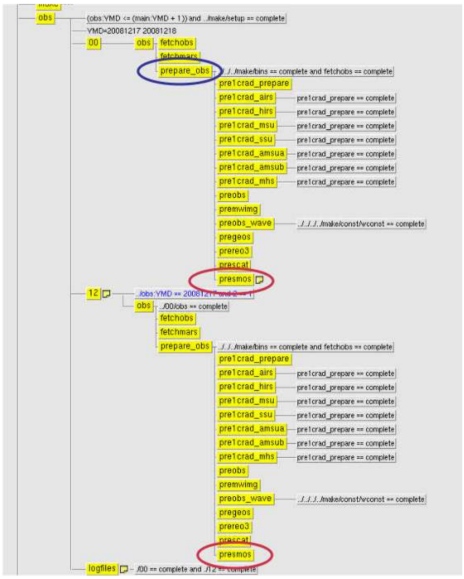

(a) SMOS preprocessing tasks in the IFS

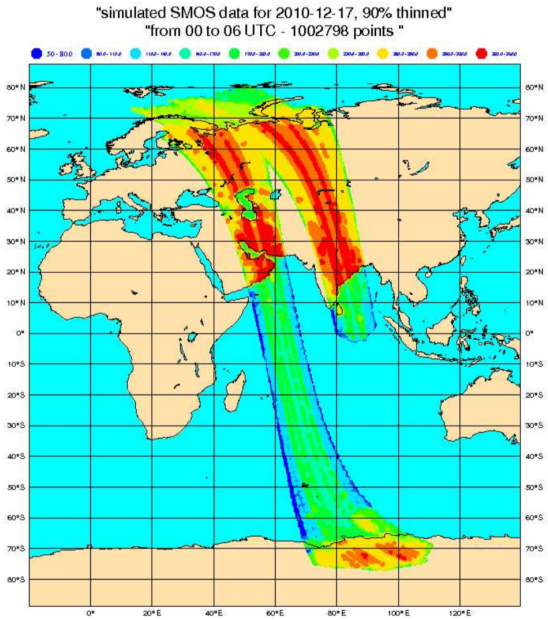

(b) Example of prototype SMOS data in the IFS

Figure 2: Implementation of SMOS in the IFS before the SMOS launch. Left panel show the IFS suite with the introduction of dedicated SMOS tasks in the observation family. Right panel shows preliminary maps obtained from the IFS ODB using simulated Level 1 NRT test data provided by ESA before the SMOS launch. Figure from MS1TN-Part 2 (Muñoz-Sabater et al., 2009)

not greater than 350 K. In this way observations affected by hard Radio Frequency Interference (RFI) are rejected. A simple data thinning was also introduced at the early stage to the mission, in IFS cycle 36r4, to make it possible for the IFS to cope with the large data volume provided by SMOS. The method used was to filter out 9 out of 10 subsets in each BUFR message, equivalent to thin the volume of the initial data set in about 90%. All SMOS data that go through the pre-screening jobs are presented to the IFS. The approach developed was to map the SMOS data into model space. It is in this space where SMOS data is collocated to the model grid at the required model resolution using the nearest neighbour technique (specific Fortran routine in the IFS, provided in the appendix of MS1TN-Part 1/2/3 by Muñoz-Sabater et al. (2010)). Figure 3 left shows the SMOS workflow in the IFS, including acquisition, BUFR reformatting, archiving on the ECMWF ECFS and MARS, preprocessing, conversion to ODB, colocation, interface to CMEM and computation of first guess departure, and feedback to the ODB for monitoring. The SMOS TB monitoring was then developed for both XX and YY polarisations and for six incidence angles (10°, 20°, 30°, 40°, 50°, 60°) and implemented very shortly after the SMOS launch, providing global maps with statistics and publication at the SMOS offline monitoring webpage that was put in place from January 2010 as shown in Figure 3 (right).
This work is fully described in the report (MS2TN-P1/2/3 , see Table 1) by Muñoz-Sabater et al. (2010) and further details on monitoring statistics and preliminary monitoring results were reported by Muñoz-Sabater et al. (2011c). These reports concluded the first contract (20244/07/I-LG) that focused on the implementation of the SMOS TB data in the IFS and the development of the SMOS TB monitoring system.

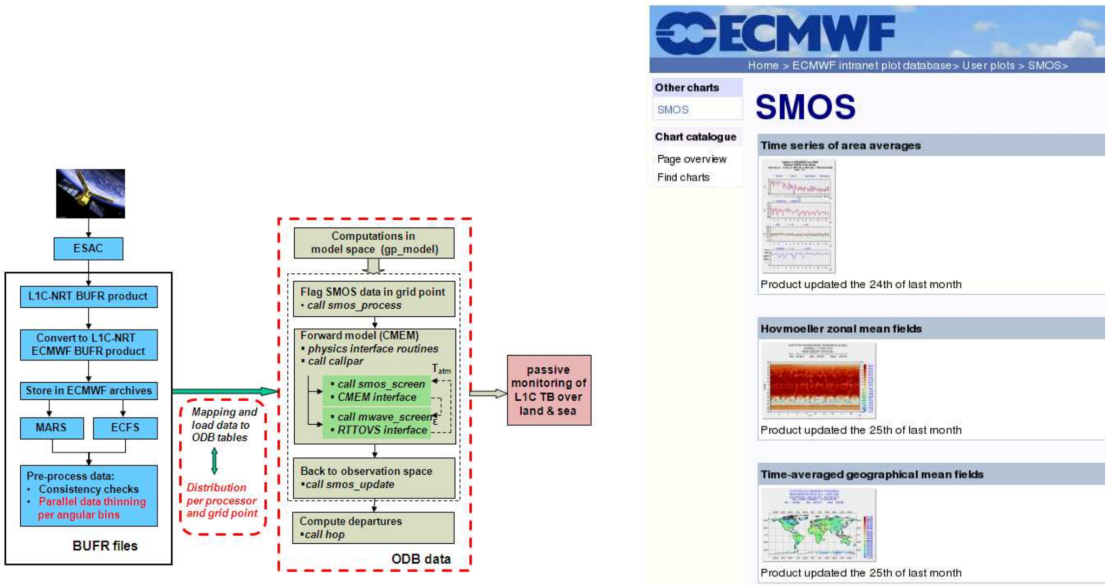

(a) SMOS preprocessing tasks in the IFS

(b) Example of prototype SMOS data in the IFS

Figure 3: SMOS monitoring implementation during the commissioning phase: organigramme of the SMOS offline monitoring running from January 2010 (left), SMOS initial monitoring web page (right). Figure from MS2TN-Part 1/2/3 Muñoz-Sabater et al. (2010).

.

3.4 SMOS real time monitoring

The framework developed during the Phase I contract, made it possible to obtain in NRT daily statistics of the observations, the model equivalent of the observations computed by CMEM in the IFS, and the difference between the two quantities, the so called first-guess departures. SMOS TB monitoring results include global maps, Hovmöller diagrams, time series and angular scatter plots on land surfaces as fully described in TN-PII-WP1100 (Muñoz-Sabater et al., 2011a) which provided a full annual cycle monitoring report. Note that a preliminary SMOS TB monitoring over ocean surfaces has also been provided, although not explicitly part of the contract, using a smooth surface emission not accounting for wind effects. Figure 4 gives an example of time series monitoring plots obtained at global scale over land pixels, for the period November 2010 to November 2011. The left panel is for XX polarisation and right panel for YY polarisation. For YY polarisation an almost systematic negative bias was observed the whole year, increasing between April and May around 4 K in absolute value. These differences were explained by snow melting impact on both the SMOS observations and the CMEM simulated TBs. At this stage of the project the snow covered areas were not filtered out and the monitoring results pointed out that they are challenging for both monitoring and assimilation. This effect was stronger for XX polarisation because CMEM is more sensitive over snow for this polarisation. A slightly larger variability of the bias is also observed on the YY polarisation.

Since the implementation of the SMOS monitoring at ECMWF nine years ago in January 2010, statistics have been continuously computed using several weeks of data. The SMOS monitoring has been a very robust way to identify systematic differences between modelled values and observations. Furthermore it also set the basis to investigate and understand the new observations before they become active in the ECMWF land assimilation scheme.

3.5 SMOS data thinning

The daily volume of SMOS data arriving at the ECMWF archives in NRT can be more than 8 Gb, which is among the greatest sources of satellite data received at ECMWF. This amount of data cannot all be introduced in the IFS for just one single satellite instrument, taking into account that data from many other satellites is used simultaneously. For SMOS, it is estimated that only 5 to 10% of the initial data volume can realistically be ingested in the IFS. Data thinning is therefore a mandatory step and also prevents redundant and poor quality observations to go through the assimilation system. In the project Phase I, a simple thinning approach was implemented in the IFS as a practical solution, consisting of keeping only 1 out of 10 observations (see Section 3.3). The SMOS data thinning was later on replaced by a flexible approach implemented in IFS cycle 37r2, which accounts for thinning configuration parameters for the input dataset in the IFS for both monitoring of brightness temperatures and assimilation experiments. Figure 5 shows resulting data volume obtained for different thinning configurations based on a 12h assimilation window. It shows that with a 6 incidence angles monitoring suite, less than 7% of the original data volume is used. Although the data reduction is important, there is still a significantly large number of observations in the SMOS ODB. By using the monitoring suite but rejecting pixels with more than 50% water content (so only keeping land points), only 4% of the total original volume remains in the IFS. If on top of that, only data within the alias-free FOV is used (of better quality) then the percentage is further reduced to 3%, corresponding to about 9% of the total data over land. This approach permits the investigation of assimilating different multi-angular configurations of the observations for the accurate access to soil moisture. It is fully described in the TN-PII-WP1200 report (Muñoz-Sabater et al., 2011d).

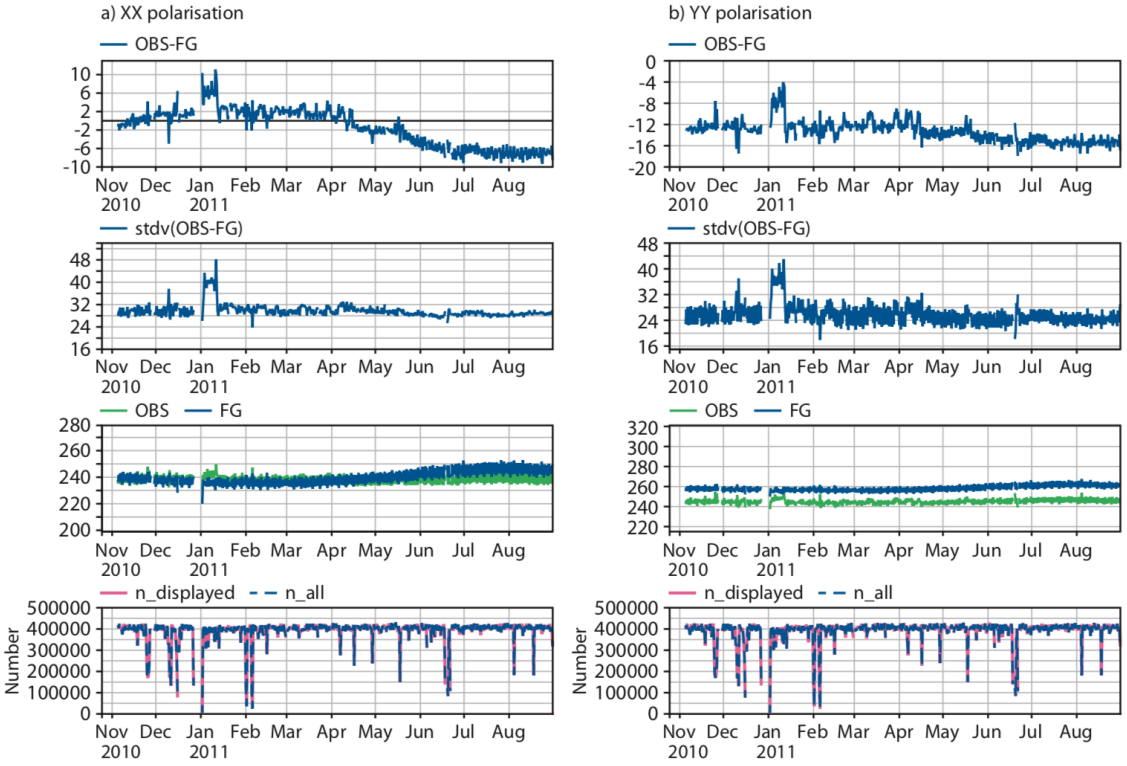

Figure 4: Global scale, time series from November 2010 to August 2011 over continental surfaces, at 40° incidence angle, of mean bias (top figures), mean standard deviation of bias (second top row), comparison between observed brightness temperatures and the CMEM modeled equivalents (third row), and number of observations (bottom figures). Each value is an averaged value per ECMWF 4DVAR 12h cycle. Left panel is for XX polarisation, right panel for YY polarisation. Figure from TN-PII-WP1100 (Muñoz-Sabater et al., 2011a).

.

All data 00Z analysis 20101201 (2100-0900)	154.364.953 (100%)
Water pixels + HHV / HVV	97.024.125 **(62.85%)**
Land pixels + AFOV	30.073.313 **(19.48%)**
Monitoring suite (6 angles +/- 0.5)	10.564.356 **(6.85%)**
Monitoring suite (6 angles +/- 0.5) + land pixels	5.983.758 (3.87% or **10.41 % over land**)
Monitoring suite (6 angles +/- 0.5) + land pixels + AFOV	4.923.337 (3.19% or **8.58% over land)**
Monitoring suite (6 angles +/- 1) + land pixel	11.979.065 (7.76% or **20.89% over land**)
Monitoring suite (6 angles +/- 2) + land pixels	23.728.031 (**15.37%** or **41.37% over land**)
Monitoring suite (6 angles +/- 3) + land pixels	35.189.567 (**22.79%** or **61.34% over land**)

Figure 5: Influence on several thinning configurations in IFS cycle 37r2, on the SMOS data volume (number of values and percent) based on SMOS data between 21h00 on 30 November 2010 and 9h00 on 1 December 2010, from TN-PII-WP1200 (Muñoz-Sabater et al., 2011d).

3.6 SMOS noise filtering

SMOS provides multi-angular measurements of polarised brightness temperatures, i.e. a region on the Earth's surface is being observed under different viewing angles Kerr et al. (2010); Mecklenburg et al. (2016). Depending on the location of the observed area within the Field Of View (FOV), the number of views can vary from a few units to several dozens. The geometry of the observation is complex, and inaccuracies in the antenna pattern estimation, radiometric resolution, bias and accuracy lead to noise in the SMOS angular observations. In addition, the same area of the Earth surface can be observed at different viewing geometries, and that can turn into quite different pixel shapes and sizes, specially at large incidence angles. Therefore a significant angular noise contribution is also due to the diverse nature of the Earth's surface. So, a crucial step in the development of SMOS TB data assimilation in the IFS was to develop, test and validate a methodology to reduce the random noise in the observations entering the data assimilation system.

The SMOS noise filtering method developed and implemented at ECMWF is based on the data angular binning. The relation between TB and incidence angle was shown to be very well described by a 2nd order polynomia. It was evaluated for the raw data as well as for data angular bins of 0.5°, 1°, 2° and 3° for points located in several areas of the world (RFI free areas in South East of Australia, North West of South America and North of North America). The impact of soil texture and vegetation characteristics was also investigated and showed that there is not any evidence of any type of soil texture or vegetation cover type over which observations are more noisy. Figure 6 gives an example of the angular dependency of TBs for different angular bins for a grid point located in South Australia corresponding to a desert area. Averaging observed brightness temperatures over the same node in angular bins of different size, the noise of the observations was reduced. Based on a larger scale analysis we found that the optimal bin size is 2° s (+/- 1°), as for this bin the polynomial regression model explains better the angular signature of the observations while decreasing the noise. From a general perspective, this method decreases noise from SMOS observed brightness temperatures by 3 K. Another advantage is that this method reduces the volume of data and also eases an operational implementation, which makes this method suitable to be implemented within the Integrated Forecasting System of ECMWF. It has been used since 2011 for both monitoring and data assimilation activities at ECMWF. The method is fully described in the TN-PII-WP1300 report (Muñoz-Sabater and de Rosnay, 2011) and in the peer reviewed article by Muñoz-Sabater et al. (2014b).

3.7 Level 3 root zone soil moisture and DA Impact

A SMOS level 3 root-zone soil moisture product was developed based on the SMOS level 1 Near Real Time (NRT) brightness temperatures assimilation in the ECMWF Simplfied Extended Kalman Filter (SEKF) (Drusch et al., 2009a; de Rosnay et al., 2013). This required significant technical work to include the SMOS data in the ECMWF SEKF. The SMOS TB data was introduced in the observation vector, with the SEKF using a block diagonal observation error with standard deviation set to the SMOS radiometric accuracy. This preliminary implementation is described in Muñoz-Sabater (2015) that presented the very first data assimilation results obtained at ECMWF with the SMOS data, using a global mean bias correction. For the root zone product a point-wise bias correction was used based on a monthly matching similar to the one described in section 3.10, but based on only 2.5 years of SMOS data and using a five month moving window to account for the seasonal cycle. These developments led to the SMOS TB data assimilation system available in IFS cycle 38r2, able to use direct satellite radiances to constraint soil moisture. Two long-term numerical experiments were conducted at a resolution of 40km (TL511), closest to the SMOS resolution for the period from 1 May 2010 to 31 October 2012, with SMOS TB assimilation (to produce the root zone product) and without SMOS assimilation (used a control experiment to evaluate the impact of SMOS). Figure 7 shows the impact of SMOS data assimilation on both soil moisture (verified against in situ data) and atmospheric forecasts (verified against own analysis). The soil moisture validation has been a key component of the soil moisture activities at ECMWF. As illustrated Figure 7 a number of soil moisture networks were used to validate the ECMWF soil moisture analysis and

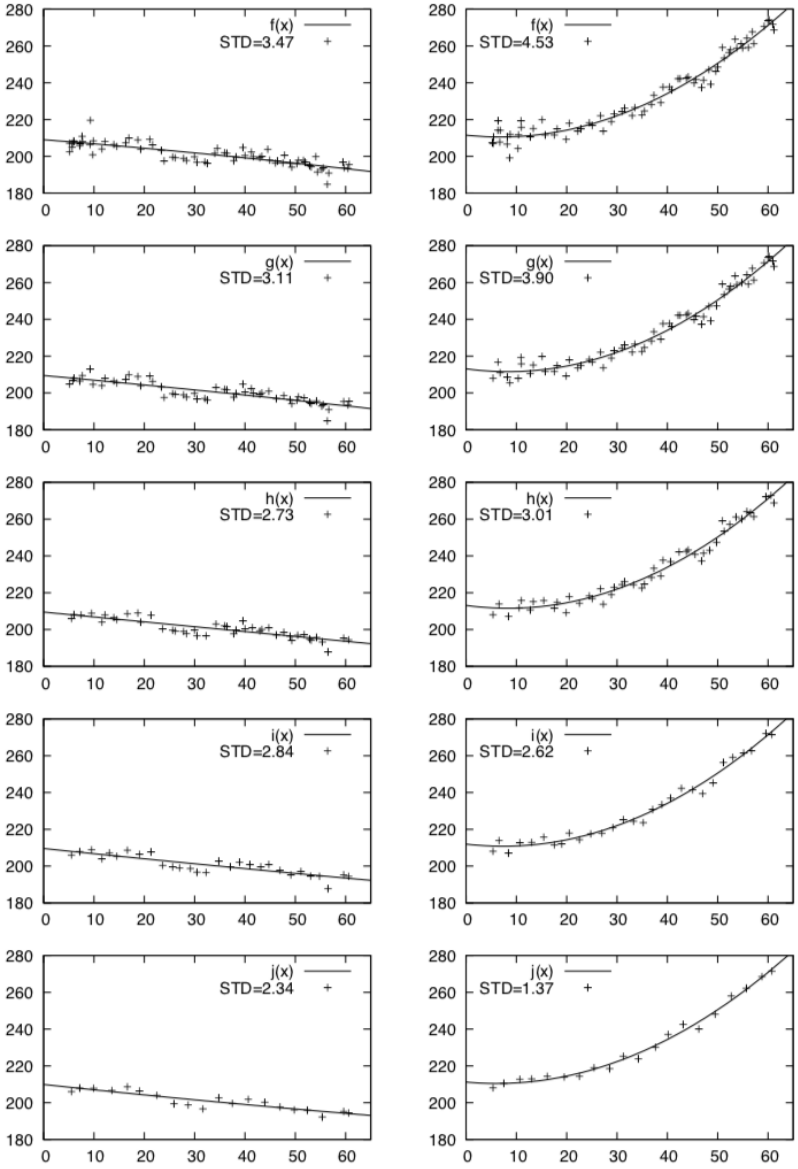

Figure 6: Relation between TB data and incidence angle for a pixel in Australia (grid id 8167123). Observations (plusses) and the 2nd order polynomial fitted curve (solid line) the 1 December 2010. Left panel is for the XX polarisation and right panel for the YY polarisation. In the top figures all the observations acquired at this grid point are included, then bins of 0.5°, 1°, 2° and 3° are applied, respectively, to average the observations. STD shows the standard deviation of the residues to the fitted curve. Figure from TN-PII-WP1300 (Muñoz-Sabater and de Rosnay, 2011).

forecasts. We do not provide the detail of the individual networks in this final report as thorough descriptions of the networks and the validation method are provided in papers by Albergel et al. (2012b,a, 2013).
Figure 7 shows that, although the system was not fully optimised yet, these results showed relatively good performances of the root zone product. The atmospheric scores suggested a decrease of the forecast error for air temperature and air humidity in the Southern Hemisphere, but an increase in the Northern Hemisphere. The overall conclusion of this important developement was to show that ECMWF had developed a functioning data assimilation system able to produce a new soil moisture product, that is based on assimilating SMOS data. It showed interesting and preliminary results, with a clear impact of SMOS data on land surface and near surface atmospheric variables. It also emphasised that deeper investigations were needed to optimise the use of these data in the IFS in synergy with other conventional and remote sensing data already used at ECMWF.

The production algorithm and the architecture of the production chain, is based on the land surface model Hydrology Tiled ECMWF Scheme for Surface Exchanges over Land (Balsamo et al., 2009), CMEM (de Rosnay et al., 2009b) and the IFS SEKF (de Rosnay et al., 2013). Detailed descriptions of assimilation system, the root zone product and preliminary assessment of SMOS TB assimilation in the IFS are provided in TN-PII-WP2000-2100 (Muñoz-Sabater et al., 2014a).

	CTRL-DA				SMOS-DA			
network	**MB**	**RMSD**	**R**	**N**	**MB**	**RMSD**	**R**	**N**
SMOSMANIA	-0.017	0.067	0.77	9	-0.017	0.063	0.74	10
AMMA	-0.117	0.131	0.56	1	-0.082	0.096	0.45	3
SCAN	-0.078	0.132	0.53	119	-0.072	0.129	0.53	119
USCRN	-0.078	0.116	0.66	69	-0.077	0.117	0.67	68
MAQU	0.027	0.067	0.75	16	0.027	0.067	0.74	16
SWATMEX	-0.077	0.091	0.82	9	-0.081	0.097	0.79	8
VAS	-0.075	0.086	0.72	2	-0.084	0.098	0.58	1
OZNET	-0.103	0.121	0.67	31	-0.103	0.121	0.70	31
REMEDHUS	-0.065	0.092	0.57	17	-0.071	0.094	0.59	18
UMBRIA	-0.153	0.159	0.65	2	-0.152	0.158	0.67	2
HOBE	-0.052	0.075	0.70	29	-0.033	0.067	0.69	30

(a)

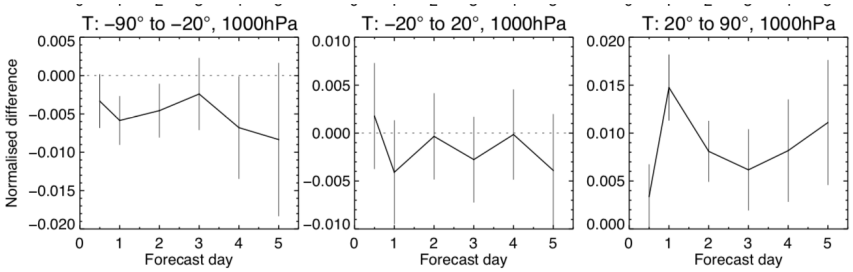

(b)

Figure 7: Results of SMOS TB assimilation in IFS cycle 38r2. Top panel: Soil moisture verification statistics of IFS experiments with (right) and without (left) SMOS TB data assimilation, against different soil moisture networks. Bottom panel: Normalized root mean square 1000hPa air temperature forecast error difference between experiments with and without SMOS TB assimilation, for June to August 2010. Forecast errors are computed against the own experiment analyses. Vertical bars show 95% confidence intervals. Left column is for the Southern Hemisphere extra tropical region, middle column for tropics and right column for Northern Hemisphere extra tropical region. Figure from TN-PII-WP2000-2100 (Muñoz-Sabater et al., 2014b).

3.8 Hot spot analysis

SMOS Hot Spots are characterised by a strong sensitivity of the SMOS data to soil moisture conditions and strong coupling between soil moisture and low level atmosphere. They are of high interest for data assimilation as SMOS is expected to have the largest impact in these areas. The SMOS Hot Spots were investigated by looking at the sensitivity of the simulated brightness temperatures to variations of soil moisture in the IFS. This corresponds to study the first component (for each incidence angle and polarisation) of the SMOS Jacobian matrix computed from perturbed IFS trajectories.

Figure 8 shows the averaged Jacobians during boreal summers, for H (left) and V (right) polarisations (in the Earth reference frame). The West-Center of the US and the Sahel regions present strong sensitivity of the model brightness temperatures to small perturbations of soil moisture. This is consistent with the large seasonal dynamical range of brightness temperatures, in response to variations of soil moisture in these areas. The model is also very sensitive in the far North of Canada, all the North of Africa and Middle East, South of Africa, in particular the Western part, Center of Asia and West-Center of Australia. The sensitivity shown by the model is notably larger for H than for V polarisation, as expected.
Interestingly, this study also showed that over desert and very dry areas of North of Africa and Middle East, the effective temperature increases significantly with increasing soil moisture. When soil moisture increases then the effective temperature sampling depth decreases too, and therefore the effective temperature gets closer to that of the surface. Since for desert areas the surface temperature is higher than the deep soil temperature (due to the strong radiative heating), then the effective temperature increases too with increasing soil moisture in the perturbed trajectories. This leads to positive Jacobian values in North Africa. This strong sensitivity over hot desert surfaces is however not expected to have any impact on SMOS data assimilation as these areas are consistently dry with very low temporal variability.
The main conclusion of this study was to show that the centre of the US and the Sahelian regions are SMOS Hot Spot areas. These areas are consistent with the soil moisture hot spots already identified by Koster et al. (2004) by a strong coupling between soil moisture and precipitation. They are characterised by strong sensitivity of SMOS brightness temperatures to soil moisture variations, large range of brightness temperatures with low to moderate LAI correspond to the SMOS Hot Spots. Results are presented and discussed in the TN-PII-WP2300 report (Muñoz-Sabater et al., 2013).

3.9 SMOS assimilation: background and observation error scenarios

In continuity with the work presented in section 3.7, further research was dedicated to refine the SMOS TB data assimilation system and in particular to investigate the sensitivity of the ECMWF soil moisture analyses to different background and SMOS brightness temperatures error scenarios in the SEKF. Using IFS cycle 40r1, a set of 1-month data assimilation experiments, with SMOS data combined or not with other types of observations, were conducted. They explored different configurations of the SMOS observation error (increasing or decreasing the confidence in the observations) and model background error representation (static or propagated in time, with or without soil texture dependence). Results of these experiments were compared against in-situ soil moisture data from the USCRN and SCAN networks in USA, and the atmospheric impact on meteorological variables was evaluated. Figure 9 depicts the atmospheric forecasts impact of SMOS data Pseudo Insertion (SMOS+PI, black curve) and SMOS assimilation with doubled observation error (SMOS+2R, red curve), compared to a reference experiment (dotted black horizontal line) were SMOS is assimilated using the radiometric accuracy as described in previous assimilation studies conducted in this project such as summarised in Section 3.7, and Muñoz-Sabater et al. (2014a).

Results of this work package were critical to design the SMOS TB assimilation observation and background error configuration. They showed in particular that assigning twice the radiometric accuracy as the SMOS

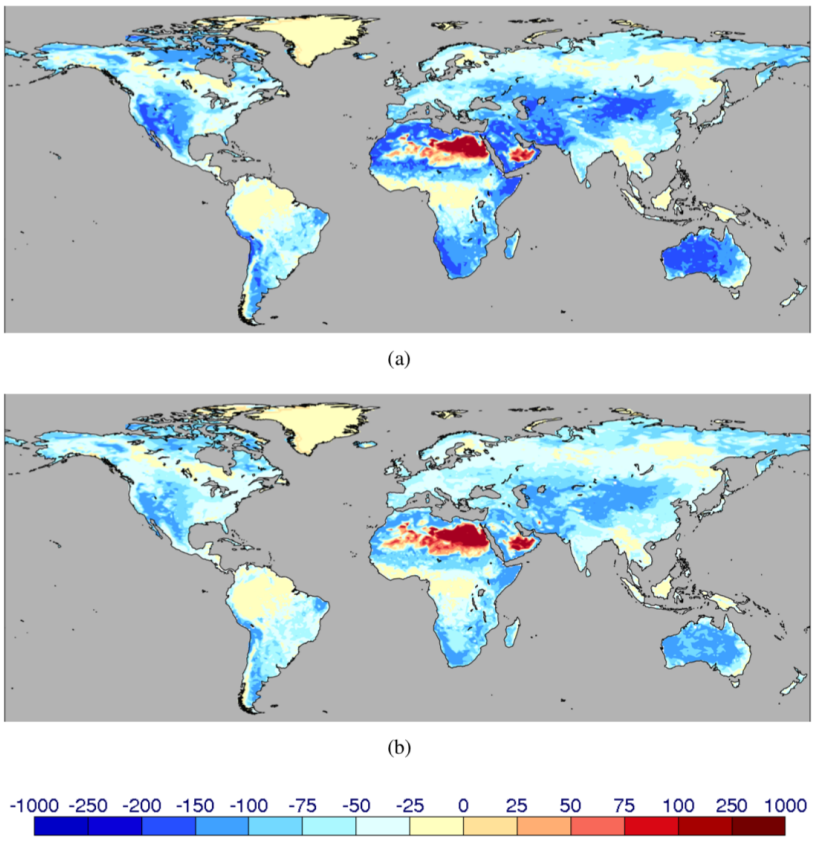

Figure 8: Averaged first component of the SMOS Jacobian (in K/m^3m^{-3}) for June, July and August 2010. Top plot is for XX polarisation and bottom plot is for YY polarisation. Figure from TN-PII-WP2300 (Muñoz-Sabater et al., 2013).

observation error had a positive impact on the temporal dynamical behaviour of the soil moisture analyses, reducing the noise in the increments. It showed that propagating the background error matrix along the assimilation window did not provide evidence of any improvement, as the size of the assimilation window and the model error introduced are too small to have a significant effect on the background error.
This work is described in detail in the TN-PII-WP3401-3402 report Muñoz-Sabater et al. (2016a) and in a publication by Muñoz-Sabater et al. (2018).

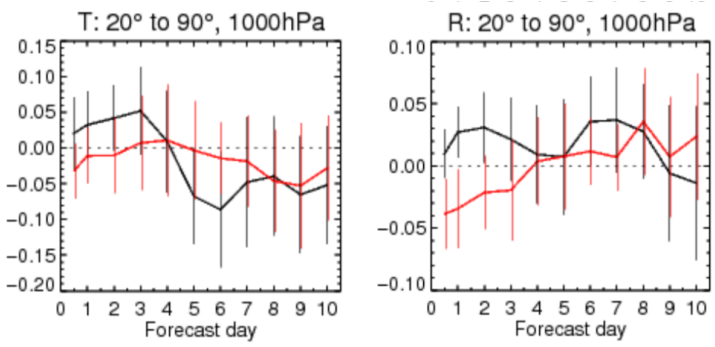

Figure 9: SMOS TB assimilation impact in IFS cycle 40r1. Air temperature (left panel) and air humidity (right panel) normalised root mean square forecast error of SMOS+PI (black curve) and SMOS+2R (red curve) experiments compared to the control SMOS experiment, as a function of the forecast lead time. Scores are shown for four different pressure levels: 1000 (bottom), 850 (middle bottom), 500 (middle top) and 200 hPa (top). The operational analyses are used as reference. Error bars show 95% confidence intervals. Figure from TN-PII-WP3401-3401 (Muñoz-Sabater et al., 2016a).

3.10 SMOS brightness temperature forward modelling, bias correction and long term monitoring at ECMWF

In support of the SMOS data assimilation developments, CMEM was continuously developed to define its optimal configuration for SMOS monitoring and data assimilation over land. Simulated brightness temperature were compared to the observed SMOS near real time reprocessed brightness temperature product for 2010-2011, for 36 configurations of CMEM using different sets of parameterisations. Results showed that simulated brightness temperatures are more sensitive to the choice of vegetation opacity and soil roughness models than to the dielectric model. Best configurations of CMEM were shown to be those using the so-called Wigneron vegetation opacity model with the simple empirical Wigneron soil roughness model. The Wang and Schmugge and the Mironov soil dielectric models perform similarly and lead to better agreement with SMOS observations than the Dobson dielectric model. Based on this intercomparison the configuration of CMEM retained for ECMWF SMOS forward modelling activities is the one based the Wang and Schmugge dielectric model, the Wigneron simple roughness model and the Wigneron vegetation model.

In parallel, the SMOS bias correction was regularly updated, providing successive improved versions of the bias correction based on improved (Cumulative Distribution Function) CDF-matching method, increased length of the available data set and improved versions of both the SMOS product and the model versions. This continuous approach supported data assimilation developments and experiments through the Contract Phase II and Phase III periods from 2012 to 2015. The latest version of the bias correction using v505 brightness temperature for 2010 to 2013 was used for the data assimilation experiments presented in Sections 3.9 and 3.11.
It uses a monthly (three months moving window) CDF correction based on SMOS and ECMWF re-analysis-based brightness temperatures for the period from 1 January 2010 to 31 December 2013 in IFS cycle 41r1.

Figure 10 illustrates the RMSE between SMOS and ECMWF forward TBs for 2013 at 40° incidence angle, before and after bias correction. As shown in de Rosnay et al. (2018), the CDF-matching efficiently corrects for systematic differences between observations and model, with global root mean square differences (RMSD) and global mean bias for 2010-2013 for 30°, 40°, 50° incidence angles decreasing from 16.7 K and -2.1 K before bias correction to 7.91K and 0.0016 K after bias correction, respectively. The monthly approach allows to correct for seasonal cycles systematic differences, with correlation values improved from 0.56 before bias correction and 0.62 after bias correction. Residual differences remaining after bias correction correspond to random differences between the model and observations which provide relevant information for monitoring and data assimilation purposes.

Long term monitoring of SMOS brightness temperature monitoring was investigated covering a 7-year period 2010-2016 at both polarisations, at 40° incidence angle using reanalysis-based forward simulations and reprocessed SMOS data. RMSD, correlation and anomaly correlation statistics displayed in Figure 10 clearly show that SMOS and ECMWF reanalysis-based brightness temperature agreement steadily improves between 2010 and 2016, indicating improvement of SMOS products quality through the SMOS lifetime.

Part of these results were presented in the paper published by Mecklenburg et al. (2016). An overview of the SMOS forward modelling activities, bias correction and long term monitoring is provided by (de Rosnay et al., 2018) and submitted for publication (de Rosnay et al., 2019a).

3.11 Assimilation of SMOS brightness temperature in the ECMWF Integrated Forecasting System

Based on the developments presented in the previous sections, a comprehensive study was conducted to assess the impact of assimilating SMOS TB alone or in combination with screen level observations and ASCAT (Advanced Scatterometer Wagner et al. (2006); Bartalis et al. (2007)) soil moisture retrievals, on land surface and near-surface atmospheric variables. Independent quality controlled in situ soil moisture observations belonging to several networks included in the International Soil Moisture Network were used to validate the quality of both the new soil moisture analyses and the skill to predict soil moisture up to 5 days ahead. The impact on atmospheric variables was evaluated through computation of the forecast skill at different lead times. The analysis period was selected around the boreal summer, a period of the year when evaporatranspiration fluxes are stronger, and when it is therefore expected that the assimilation of remote sensing data provides the largest impact on the state of the soil. Figure 11 (top) gives soil moisture validation statistics for different configurations of the observing system were the IFS is not analysing soil moisture, or using SMOS data with and without ASCAT and screen level variables (SLV). These results showed that the soil moisture state benefits from the direct assimilation of SMOS TB, especially in better representing the temporal variations of soil moisture in time. Figure 11 presents the impact on the atmospheric forecasts. It shows that the skill on atmospheric variables is mainly driven by the screen level observations.
The main conclusion is that despite the clear benefits on the soil state, SMOS TB data need to be used with screen level variables to add value on the state of the atmosphere. This results points to inconsistencies in the physical coupling between the land and near-surface components of the ECMWF Earth system and support further model developements.

This study (TR3PIII-WP4040) is presented in the paper submitted for publication in the Quarterly Journal of Royal Meteorological Society Muñoz-Sabater et al. (2019).

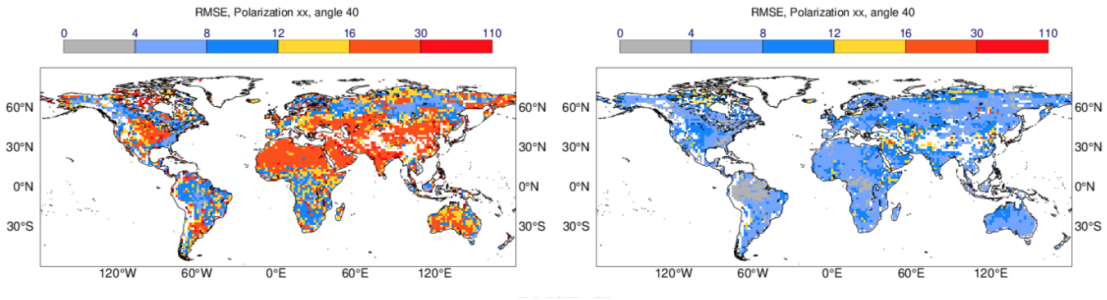

(a) Bias correction impact on TB RMSE (K)

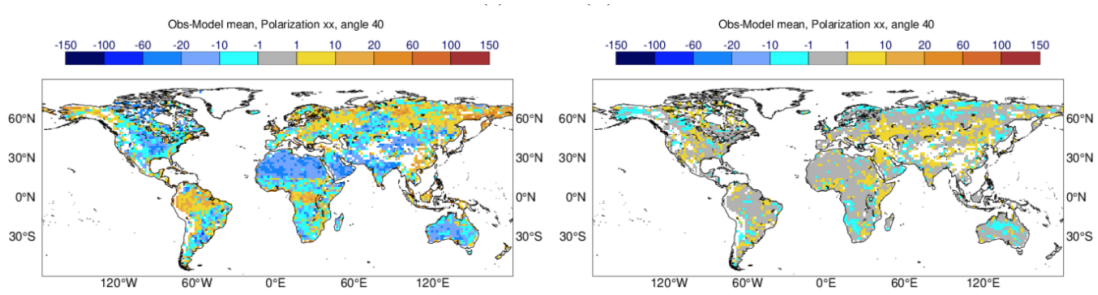

(b) Bias correction impact on TB Bias (K)

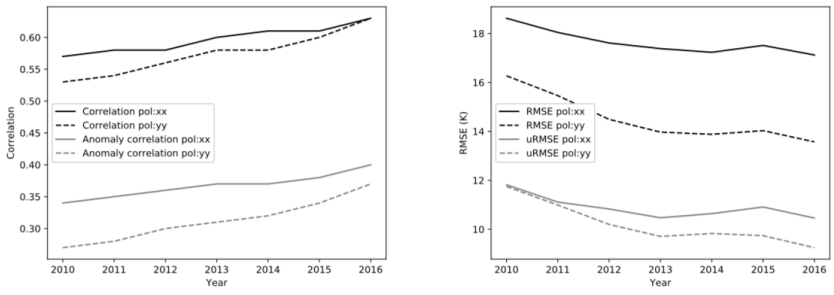

(c) SMOS long term monitoring

Figure 10: Top and middle panel: Comparison between ECMWF CMEM and SMOS brightness temperatures before (left) and after (right) bias correction for 2013 XX pol and 40° incidence angle. Panels a and b show RMSE (K) and bias (K), respectively. Bottom panel: Global mean statistics of SMOS brightness temperatures monitoring from 2010 to 2016, comparing SMOS observations to ECMWF CMEM reanalysis of L-Band brightness temperature, at 40° incidence angle, at XX (solid line) and YY (dashed line) polarisations. Left panel show correlation (black) and anomaly correlation (grey). Right panel shows RMSE (black) and uRMSE (grey). Figure from MS3TN-Part2 (de Rosnay et al., 2018).

		surface				root-zone		
		ubRMSD	R	an_R	N	ubRMSD	R	N
REMEDHUS	OL	0.053	0.72 (0.12)	0.42 (0.16)	17			
		0.049	0.72 (0.12)	0.50 (0.12)	15			
	SLV	0.052	0.74 (0.08)	**0.56 (0.16)**	17			
		0.049	0.68 (0.07)	**0.55 (0.12)**	15			
	ASCAT	**0.045**	0.69 (0.12)	0.45 (0.13)	17			
		0.047	0.68 (0.10)	0.42 (0.09)	15			
	SMOS	0.049	**0.77 (0.12)**	0.54 (0.13)	17			
		0.050	**0.73 (0.14)**	0.46 (0.09)	15			
	SMAS	0.048	0.72 (0.09)	0.49 (0.13)	17			
		0.046	0.71 (0.05)	0.42 (0.10)	15			
	SLVSMAS	0.055	0.74 (0.08)	0.48 (0.11)	17			
		0.048	0.66 (0.07)	0.45 (0.11)	15			
SMOSMANIA	OL	0.049	0.78 (0.08)	0.62 (0.11)	11	0.030	0.85 (0.09)	11
		0.049	0.84 (0.08)	0.62 (0.14)	10	0.032	0.89 (0.06)	10
	SLV	0.048	0.75 (0.12)	0.61 (0.10)	11	**0.029**	0.82 (0.08)	11
		0.049	0.83 (0.11)	0.55 (0.14)	10	**0.031**	0.89 (0.06)	10
	ASCAT	0.047	**0.80 (0.06)**	0.64 (0.15)	11	0.035	0.84 (0.06)	11
		0.052	0.85 (0.08)	0.59 (0.12)	10	0.034	**0.90 (0.06)**	10
	SMOS	**0.044**	**0.80 (0.09)**	**0.65 (0.12)**	11	0.031	0.86 (0.12)	11
		0.049	**0.86 (0.09)**	**0.62 (0.10)**	10	0.032	**0.90 (0.07)**	10
	SMAS	0.046	**0.80 (0.07)**	**0.65 (0.12)**	11	0.031	0.86 (0.08)	11
		0.050	0.84 (0.10)	**0.62 (0.12)**	10	0.032	**0.90 (0.06)**	10
	SLVSMAS	0.047	0.74 (0.09)	0.64 (0.14)	11	0.031	**0.89 (0.09)**	11
		0.047	0.80 (0.09)	0.59 (0.11)	10	**0.031**	0.88 (0.10)	10

(a) SMOS TB data assimilation impact on soil moisture

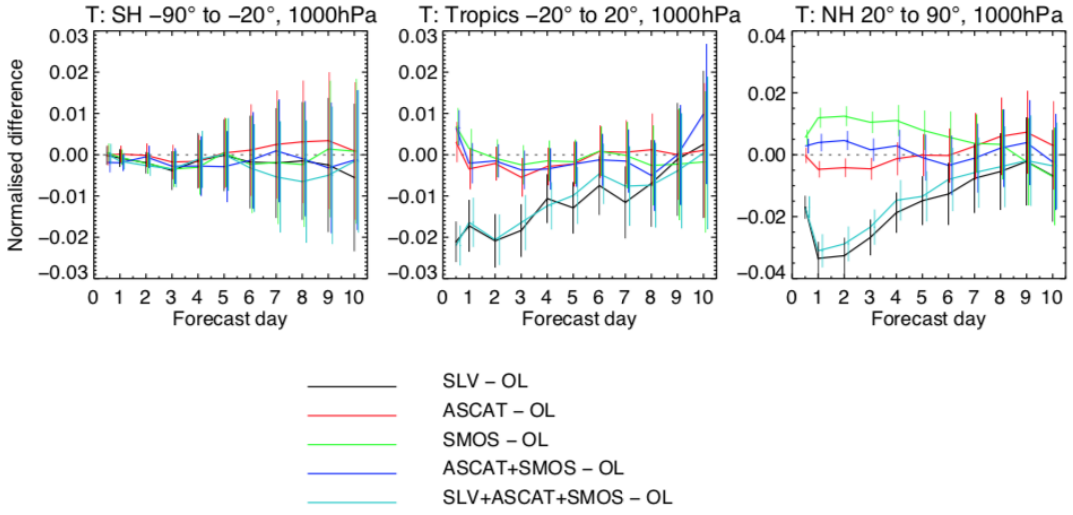

(b) SMOS TB data assimilation impact on atmospheric forecasts

Figure 11: Impact of SMOS TB data in IFS cycle 41r1. Top panel: Soil moisture validation statistics for different networks and experiments, for May-Sept. 2012 and 2013 (top and second line of each experiment, respectively). Values in parenthesis represent the estimated uncertainty. Bold-face values show best scores for each year and metric. N represent the number of stations with statistically significant values. Bottom panel: Normalised RMS forecast error of the 1000 hPa air temperature for May-Sept 2012-2013 for the Southern Hemisphere (left column), Tropics (middle column) and Northern Hemisphere (right column). The black (SLV), red (ASCAT), green (SMOS), dark blue (SMAS) and light blue (SLVSMAS) experiments are shown. The reference is an OL (Open Loop) experiment which has no soil moisture assimilation. Form TR3PIII-WP4040 (Muñoz-Sabater et al., 2019).

4 Conclusion

The SMOS DA study has been a very successful activity at ECMWF. The SMOS NRT TB observations were implemented in the IFS, starting for the SMOS NRT product BUFR definition and approval by the World Meteorological Organizaton (WMO), the development of the SMOS Observation Data Base at ECMWF, SMOS acquisition, preprocessing, noise filtering, data thinning, etc... The SMOS forward operator, CMEM was developed by ECMWF. It is an open source code, freely available from the ECMWF web page under an Apache licence, benefiting a large hydrological and meteorological community, for low frequency passive microwave applications over land and in particular for SMOS and SMAP aplications. SMOS data was implemented in the IFS and SMOS TB monitoring started at a very early stage of the mission in January 2010. SMOS TB data has been continuously monitored since then, and it will continue for the SMOS lifetime which we hope to be as long as possible hopefully in in the next decade. The SMOS bias correction was continuously developed, benefiting from increasing SMOS times series available as the mission was producing data. It was conducted in support of the SMOS data assimilation developments from 2010 to 2016. The SMOS TB data assimilation development was a major activity that required both scientific and technical research and developments. SMOS TB data was introduced in the ECMWF SEKF observation vector, the SMOS Jacobians were thoroughly investigated (hot-spot analysis), and the observations and background errors configuration was studied and defined, leading to progressive improvement of the SMOS TB DA performances.

This project provided an outstanding contribution to the ECMWF land assimilation developments. It was very productive in term of publications with 20 reports and 25 peer reviewed article related to SMOS TB activities over land. The main outcomes of this study is to demonstrate the relevance of the SMOS observations for numerical weather prediction applications. Long term monitoring and assimilation results also open also perspectives for SMOS data assimilation studies for environmental systems monitoring, prediction and long term reanalyses.

Acknowledgements

This work was funded under the ESA-ESRIN contracts number 20244/07/I-LG and 4000101703/10/NL/FF/fk. We thank Matthias Drusch and Susanne Mecklenburg for their contribution in the project definition. Many thanks to Raffaele Crapolicchio for fruitful discussions and interactions about the SMOS PDGS interface and IFS products dissemination. Thanks to the SMOS QWG team and to the CESBIO colleagues, in particular Philippe Richaume and Yann Kerr, for the useful interactions around the ECMWF and SMOS products and RFI filtering. Special thanks to Nemesio Rodrìguez Fernàndez for lively SMOS discussions when he was at ECMWF to work on the neural network project. Thanks to all the external collaborators who contributed to CMEM development and validation, including Jean-Pierre Wigneron, Marie Parrens, Jan Polcher and Martin Lange. Also thanks to many ECMWF staff members who have contributed to this work, in particular Souhail Boussetta and Gianpaolo Balsamo for their advice regarding H-TESSEL and soil moisture interaction with the atmosphere, Ioannis Mallas for the SMOS observation acquisition, Mohamed Dahoui for the SMOS monitoring implementation.

References

Albergel, C., Balsamo, G., de Rosnay, P., Muñoz-Sabater, J., and Boussetta, S. (2012a). A bare ground evaporation revision in the ECMWF land-surface scheme: evaluation of its impact using ground soil moisture and satellite microwave data. *Hydrology and Earth System Sciences*, 16:3607–3620. 10.5194/hess-16-3607-2012.

Albergel, C., de Rosnay, P., C., G., Muñoz-Sabater, J., Hasenauer, S., Isaksen, L., Kerr, Y., and Wagner, W. (2012b). Evaluation of remotely sensed and modelled soil moisture products using global ground-based in-situ observations. *Remote sens. environ.*, 18:215–226. doi:10.1016/j.rse.2011.11.017.

Albergel, C., Dorigo, W., Reichle, R. H., Balsamo, G., de Rosnay, P., Muñoz-Sabater, J., Isaksen, L., de Jeu, R., and Wagner, W. (2013). Skill and Global trend analysis of soil moisture from reanalyses and microwave remote sensing. *J. Hydrometeo*, 14:1259–1277. doi:10.1175/JHM-D-12-0161.1.

Balsamo, G., Viterbo, P., Beljaars, A., van den Hurk, B., Hirsch, M., Betts, A., and Scipal, K. (2009). A revised hydrology for the ECMWF model: Verification from field site to terrestrial water storage and impact in the Itegrated Forecast System. *J. Hydrometeo*, 10:623–643.

Bartalis, Z., Wagner, W., Naeimi, V., Hasenauer, S., Scipal, K., Bonekamp, H., Figa, J., and Anderson, C. (2007). Initial soil moisture retrievals from the METOP-A advanced scatterometer (ASCAT). *Geophys. Res. Let.*, 34. doi:10.1029/2007GL031088.

Carrera, M., Bèlair, S., and B., B. (2015). The canadian land data assimilation system (caldas): Description and synthetic evaluation study. *J. Hydrometeo*, 16:1293–1314. doi:10.1175/JHM-D-14-0089.1.

De Chiara, G. and English, S. (2016). SMOS Hurricane wind speed analysis. *ECMWF ESA contract report*. ESA contract 4000101703/10/NL/FF/fk, TR5PIII-WP4060.

de Rosnay, P., Dragosavac, M. ., Drusch, M., Gutiérrez, A., Rodríguez Lõpez, M., Wright, N., Muñoz-Sabater, J., and Crapolicchi, R. (2012). SMOS NRT BUFR Specification v2.0. *ECMWF and ESA/ESRIN*. ECMWF and ESA/ESRIN.

de Rosnay, P., Drusch, M., Boone, A., Balsamo, G., Decharme, B., Harris, P., Kerr, Y., Pellarin, T., Polcher, J., and Wigneron, J.-P. (2009a). Microwave Land Surface modelling evaluation against AMSR-E data over West Africa. The AMMA Land Surface Model Intercomparison Experiment coupled to the Community Microwave Emission Model (ALMIP-MEM). *J. Geophys. Res*, 114. doi:10.1029/2008JD010724.

de Rosnay, P., Drusch, M., and Muñoz-Sabater, J. (2009b). SMOS Global Surface Emission Model. *ECMWF ESA Contract Report*. ESA/ESRIN Contract Contract 20244/07/I-LG, MS1TN-Part1.

de Rosnay, P., Drusch, M., Vasiljevic, D., Balsamo, G., Albergel, C., and Isaksen, L. (2013). A simplified Extended Kalman Filter for the global operational soil moisture analysis at ECMWF. *Quart. J. Roy. Meteorol. Soc.*, 139:1199–1213. doi: 10.1002/qj.2023.

de Rosnay, P., Muñoz-Sabater, J., Albergel, C., Isaksen, L., and English, S. (2018). SMOS brightness temperature forward modelling, bias correction and long term monitoring at ECMWF. *ECMWF ESA Contract Report*. ESA/ESRIN Contract 4000101703/10/NL/FF/fk, MS3 Technical Note - Part2.

de Rosnay, P., Muñoz-Sabater, J., Albergel, C., Isaksen, L., English, S., Drusch, M., and Wigneron, J.-P. (2019a). SMOS brightness temperature forward modelling and long term monitoring at ECMWF. *Remote sens. environ.* submitted.

de Rosnay, P., Muñoz-Sabater, J., Albergel, C., Lawrence, H., Isaksen, L., and English (2019b). Final Report on SMOS brightness temperature activities over land: Monitoring and Data Assimilation. *ECMWF ESA Contract Report*. ESA/ESRIN Contract 4000101703/10/NL/FF/fk, FR.

Drusch, M., Holmes, T., de Rosnay, P., and Balsamo, G. (2009a). Comparing ERA-40 based L-band brightness temperatures with Skylab observations: A calibration / validation study using the Community Microwave Emission Model. *J. Hydrometeo*. in press, doi: 10.1175/2008JHM964.1.

Drusch, M., Scipal, K., de Rosnay, P., Balsamo, G., Andersson, E., Bougeault, P., and Viterbo, P. (2009b). Towards a Kalman filter based soil moisture analysis system for the operational ECMWF Integrated Forecast System. *Geophy. Res. Letters*. doi:10.1029/2009GL037716.

Flati, A., de la Fuente, A., and de Rosnay, P. (2013). Ecmwf smos dpgs interface. XSMS-GSEG-EOPG-ID-06-0002_SMOS_ECMWF_DPGS_ICD_44_01-21-13.

Holmes, T., Drusch, M., Wigneron, J.-P., and de Jeu, R. (2008). A global simulation of microwave emission: Error structures based on output from ECMWFs operational Integrated Forecast System. *IEEE Trans. Geosc. Remote Sens.*, 46(3):846–856.

Kerr, Y. H., Waldteufel, P., Wigneron, J.-P., Cabot, F., Boutin, J., Escorihuela, M., Font, J., Reul, N., Gruhier, C., Juglea, S., Delwart, S., Drinkwater, M., Hahne, A., Martin-Neira, M., and Mecklenburg, S. (2010). The SMOS mission: new tool for monitoring key elements of the global water cycle. *Proceedings of the IEEE*, 98(5):666–687. doi:10.1109/JPROC.2010.2043032.

Kerr, Y. H., Waldteufel, P., Wigneron, J.-P., Martinuzzi, J.-M., Font, J., and Berger, M. (2001). Soil moisture retrieval from space: The soil moisture and ocean salinity (smos) mission. *IEEE Trans. Geosc. Remote Sens.*, 39 (8):1729–1735.

Koster, R. D., Dirmeyer, P., Guo, Z., Bonan, G., Cox, P., Gordon, C., Kanae, S., Kowalczyk, E., Lawrence, D., Liu, P., Lu, C., Malyshev, S., McAvaney, B., Mitchell, K., Mocko, D., Oki, T., Oleson, K., Pitman, A., Sud, Y., Taylor, C., Verseghy, D., Vasic, R., Xue, Y., and Yamada, T. (2004). Regions of strong coupling between soil moisture and precipitation. *Sciences*, 305:1138–1140.

Lievens, H., Al Bitar, A., Verhoest, N., Cabot, F., De Lannoy, G., Drusch, M., Dumedah, G., Hendricks Franssen, H., Kerr, Y., Tomer, S., Martens, B., Merlin, O., Pan, M., , van den Berg, M., Vereecken, H., Walker, J., Wood, E., and Pauwels, V. (2015). Optimization of a Radiative Transfer Forward Operator for Simulating SMOS Brightness Temperatures over the Upper Mississippi Basin. *J. Hydrometeo*, 16:1109–1134.

Mecklenburg, S., Drusch, M., Kaleschke, L., Rodríguez-Fernández, N., Reul, N., Kerr, Y., Font, J., Martin-Neira, M., Oliva, R., Daganzo-Eusebio, E., Grant, J., Sabia, R., Macelloni, G., Rautiainen, K., Fauste, J., de Rosnay, P., Muñoz-Sabater, J., Verhoest, N., Lievens, H., Delwart, S., Crapolicchio, R., de la Fuente, A., and Kornbe, M. (2016). ESA's Soil Moisture and Ocean Salinity mission: From science to operational applications. *Remote sens. environ.*, 180:3–18. doi:10.1016/j.rse.2015.12.025.

Muñoz-Sabater (2015). Incorporation of microwave passive brightness temperatures in the ECMWF soil moisture analysis. *Remote Sensing*, 7(5):5758–5784.

Muñoz-Sabater, J., Dahoui, M., de Rosnay, P., and Isaksen, L. (2011a). SMOS Monitoring Report Number 2: Nov 2010 - Nov 2011. *ECMWF ESA contract report*. ESA/ESRIN Contract 4000101703/10/NL/FF/fk, TNPII WP1100.

Muñoz-Sabater, J. and de Rosnay, P. (2011). SMOS Report on noise filtering. *ECMWF ESA contract report*. ESA/ESRIN Contract 4000101703/10/NL/FF/fk, TNPII WP1300.

Muñoz-Sabater, J., de Rosnay, P., Albergel, C., and Isaksen, L. (2014a). SMOS Report on Level 3 root zone soil moisture and DA Impact SMOS. *ECMWF ESA contract report*. ESA/ESRIN Contract 4000101703/10/NL/FF/fk, TNPII WP2000-2100.

Muñoz-Sabater, J., de Rosnay, P., Albergel, C., and Isaksen, L. (2016a). SMOS report on background and observation error senarios. *ECMWF ESA contract report*. ESA/ESRIN Contract 4000101703/10/NL/FF/fk, TNPII WP3401 and WP3402.

Muñoz-Sabater, J., de Rosnay, P., Albergel, C., and Isaksen, L. (2018). Sensitivity of soil moisture analyses to contrasting background and observation error scenarios. *Water*, 10(7).

Muñoz-Sabater, J., de Rosnay, P., and Balsamo, G. (2011b). Sensitivity of L-band NWP forward modelling to soil roughness. *Int J. of Remote Sensing*. doi:10.1080/01431161.2010.507260.

Muñoz-Sabater, J., de Rosnay, P., and Dahoui, M. (2011c). SMOS continuous Monitoring Part1. *ECMWF ESA contract report*. ESA/ESRIN Contract 20244/07/I-LG.

Muñoz-Sabater, J., de Rosnay, P., and Fouilloux, A. (2010). Operational Pre-processing chain, Collocation software development and Offline monitoring suite. *ECMWF ESA contract report*. ESA/ESRIN Contract 20244/07/I-LG, MS2TN-Part1/2/3.

Muñoz-Sabater, J., de Rosnay, P., Fouilloux, A., Dragosavac, M., and Hofstadler, A. (2009). IFS interface. *ECMWF ESA contract report*. ESA/ESRIN Contract 20244/07/I-LG, MS1TN-Part 2.

Muñoz-Sabater, J., de Rosnay, P., and Isaksen, L. (2013). Hot-Spot analysis. *ECMWF ESA contract report*. ESA/ESRIN Contract 4000101703/10/NL/FF/fk, TNPII WP2300.

Muñoz-Sabater, J., de Rosnay, P., Jiménez, C., Isaksen, L., and Albergel, C. (2014b). SMOS brightness temperatures angular noise: characterization, filtering and validation. *IEEE Transactions on Geoscience and Remote Sensing*, 52(9):5827–5839.

Muñoz-Sabater, J., Lawrence, H., Albergel, C., de Rosnay, P., Isaksen, L., Drusch, M., Kerr, Y., and Mecklenburg, S. (2019). Assimilation of SMOS brightness temperature in the ECMWF Integrated Forecasting System. submitted, QJRMS.

Muñoz-Sabater, J., Rodríguez-Fernández, N., Richaume, P., Albergel, C., de Rosnay, P., and Kerr, Y. (2016b). SMOS Near-Real-Time Soil Moisture processor: Operational chain and evaluation . *ECMWF ESA contract report*. ESA contract 4000101703/10/NL/FF/fk, TR2PIII-WP4020.

Muñoz-Sabater, J., Wilhelmsson, T., de Rosnay, P., and Isaksen, L. (2011d). SMOS Report on data thinning. *ECMWF ESA contract report*. ESA/ESRIN Contract 4000101703/10/NL/FF/fk, TNPII WP1200.

Rodríguez-Fernández, N., de Rosnay, P., Albergel, C., Aires, F., Prigent, C., Richaume, P., Kerr, Y., and Muñoz Sbater, J. (2017a). SMOS SMOS Neural Network Soil Moisture Data Assimilation. *ECMWF ESA contract report*. ESA/ESRIN Contract 4000101703/10/NL/FF/fk, TR1PIII-WP4010.

Rodríguez-Fernández, N., Muñoz-Sabater, J., Richaume, P., de Rosnay, P., Kerr, Y., Albergel, C., Drusch, M., and Mecklenburg, S. (2017b). SMOS near-real-time soil moisture product: processor overview and first validation results. *Hydrology and Earth System Sciences*, 21:5201–5216.

Rodríguez-Fernández, N., Richaume, P., Muñoz Sbater, J., de Rosnay, P., and Kerr, Y. (2016). SMOS Near-real-Time Soil Moisture processor: recommended neural network configuration and algorithm description. *ECMWF ESA contract report*. ESA/ESRIN Contract 4000101703/10/NL/FF/fk, WP4020 SO-TN-CB-GS-0049.

Tietsche, S. and Balmaseda, M. (2016). Sea-ice thickness from SMOS. *ECMWF ESA contract report*. ESA contract 4000101703/10/NL/FF/fk, TR4PIII-WP4050.

Wagner, W., Naeimi, V., Scipal, K., de Jeu, R., and Martínez-Fernández, J. (2006). Soil moisture from operational meteorological satellites. *Hydrogeology Journal*, page accepted.

A Reports and publications

The SMOS TB monitoring and data assimilation study conducted at ECMWF between 2007 and 2018 conducted to a number of publications and reports. Some of them, related to work package deliverables were cited in the sections above. In addition to the deliverables, many more publications directly related to this project were produced around the SMOS forward operator and data assimilation, involving ECMWF internal and external collaborations. The table below summarises the number and type of publications (excluding SMOS NN and SMOS ocean activities) produced during the SMOS study at ECMWF:

ESA reports an deliverables	ECMWF Technical Memorandum	ECMWF Newsletter articles	Peer reviewed papers	
			directly related	external collaborations
11	7	2	11+2 submitted	12

The detailed list is given in the following two sub-sections.

A.1 Reports, Memorandums and Newsletter articles

The following ESA reports, ECMWF Technical Memorandums, ECMWF Newsletter articles were published (excluding SMOS NN and SMOS ocean activities):

1. de Rosnay P, J. Muñoz-Sabater, C. Albergel, L. Isaksen: Milestone 3 Tech Note / Part 2: SMOS brightness temperature forward modelling, bias correction and long term monitoring at ECMWF, December 2018
2. Muñoz-Sabater J., P. de Rosnay, C. Albergel, L. Isaksen: SMOS Report on background and observation error scenarios, ESA ESRIN contract 400010170310NLFFfk TNPII WP3401-3402, 2016
3. Muñoz-Sabater J., P. de Rosnay, C. Albergel, L Isaksen: SMOS Report on Level 3 root zone soil moisture and DA Impact, ESA ESRIN Contract 400010170310NLFFfk, Technical Note - Phase-II WP2000 and WP2100, February 2014
4. Muñoz-Sabater J., P. de Rosnay, C. Jimenez, L. Isaksen and C. Albergel: SMOS brightness temperatures angular noise: characterization, filtering and validation. ECMWF Technical Memorandum 715, December 2013
5. Muñoz-Sabater J., P. de Rosnay, L. Isaksen: Hot Spot Analysis ESA ESRIN Contract 400010170310NLFFfk Technical Note Phase II WP 2300, 2013
6. Albergel C., G. Balsamo, P. de Rosnay P., J. Muñoz-Sabater, and S. Boussetta: A bare ground evaporation revision in the ECMWF land-surface scheme: evaluation of its impact using ground soil moisture and satellite microwave data, ECMWF Technical Memorandum 685, September 2012,
7. Albergel C., P. de Rosnay, C. Gruhier, J. Muñoz Sabater, S. Hasenauer, L. Isaksen, Y. Kerr, W. Wagner: Evaluation of remotely sensed and modelled soil moisture products using global ground-based in situ observations, ECMWF Technical Memorandum 652, October 2011
8. Muñoz Sabater J., P.de Rosnay, M. Dahoui: SMOS continuous monitoring report - Part 1; February 2011
9. Muñoz Sabater J. and P. de Rosnay"SMOS report on noise filtering", Technical Note - Phase-II-WP1300 ESA ESRIN, 2011
10. Muñoz Sabater J., de Rosnay P. and Fouilloux A.: Use of SMOS data at ECMWF; ECMWF Newsletter no 127, pp23-27, 2011
11. Muñoz Sabater J., M. Dahoui, P. de Rosnay, L. Isaksen: Technical Note, Phase II, WP1100: SMOS Monitoring Report; Dec 2011

12. Muñoz Sabater J., T. Wilhelmsson, P. de Rosnay and L. Isaksen SMOS Report on data thinning - Technical Note - Phase II - WP1200; September 2011

13. Muñoz Sabater, J., de Rosnay, P. and G. Balsamo, 2010: Sensitivity of L-Band NWP forward modelling to soil roughness, ECMWF Technical Memorandum 624, April 2010

14. Muñoz Sabater J., P.de Rosnay, A.Fouilloux: Milestone 2 Tech Note - Parts 1/2/3: Operational Pre-processing chain, Collocation software development and Offline monitoring suite, December 2010

15. de Rosnay, P., M. Drusch and J. Muñoz Sabater: Milestone 1 Tech Note - Part 1: SMOS Global Surface Emission Model November 2009

16. Muñoz Sabater J., P.de Rosnay, A.Fouilloux, M. Dragosavac and A.Hofstadler: Milestone 1 Tech Note - Part 2: IFS Interface November 2009

17. de Rosnay, P., M. Drusch, A. Boone, G. Balsamo, B. Decharme, P. Harris, Y. Kerr, T. Pellarin, J. Polcher, J.-P. Wigneron, 2008: The AMMA Land Surface Model Intercomparison Experiment coupled to the Community Microwave Emission Model: ALMIP-MEM, ECMWF Technical Memorandum 565, July 2008

18. de Rosnay P., M. Drusch, T. Holmes, G. Balsamo, K. Scipal, E. Andersson, P. Bougeault, "ECMWF's contribution to the SMOS mission" European Centre for Medium-Range Weather Forecasts Newsletter No 115, Spring 2008

19. Drusch, M., T. Holmes, P. de Rosnay and G. Balsamo: Comparing ERA-40 based L-band brightness temperatures with Skylab observations: A calibration / validation study using the Community Microwave Emission Model ECMWF Technical Memorandum 566, July 2008

20. Drusch, M., K. Scipal, P. de Rosnay, G. Balsamo, E. Andersson, P. Bougeault and P. Viterbo Exploitation of satellite data in the surface analysis, ECMWF Technical Memorandum 576, October 2008

A.2 Peer reviewed articles

The SMOS activities related to monitoring and assimilation of TBs over land also led to the following peer reviewed articles (excluding SMOS NN and SMOS ocean activities):

1. Muñoz Sabater, J., H. Lawrence, C. Albergel, P. de Rosnay, L. Isaksen, M. Drusch Y. Kerr and S. Mecklenburg: Assimilation of SMOS brightness temperature in the ECMWF IFS, submitted Quart. J. Roy. Meteorol. Soc., 2019

2. de Rosnay P, J. Muñoz-Sabater, C. Albergel, L. Isaksen and J.P. Wigneron: SMOS brightness temperature forward modelling and long term monitoring at ECMWF, submitted Remote Sensing of Environment, 2019

3. Muñoz Sabater, J., P. de Rosnay, C. Albergel and L. Isaksen: Sensitivity of soil moisture analyses to contrasting background and observation error scenarios, MPDI Water. 10(7), 890, 2018

4. Barella-Ortiz A., J. Polcher, P. de Rosnay, M. Piles and E. Gelati: Comparison of measured brightness temperatures from SMOS with modelled ones from ORCHIDEE and H-TESSEL over the Iberian Peninsula. Hydrol Earth Syst. Sci. 21, 357-375, 2017

5. Rodríguez-Fernández N., J. Muñoz Sabater, P. Richaume, P. de Rosnay, Y. Kerr, C. Albergel, M. Drusch, and S. Mecklenburg: SMOS near real time soil moisture product: processor overview and first validation results. Hydrol and Earth Sci Syst.

6. Wigneron J.-P., T. J. Jackson , P. O'Neill , G. De Lannoy , P. de Rosnay , J. P. Walker , P. Ferrazzoli, V Mironov, S. Bircher, J. P. Grant, M. Kurum, M. Schwank, J. Muñoz-Sabater, N. Das, A. Royer, A. Al-Yaari, A. Al Bitar, R. Fernandez-Moran, H. Lawrence, A. Mialon, M. Parrens, P. Richaume, S. Delwart, Y. Kerr: Modelling the passive microwave signature from land surfaces: a review of recent results and application to the SMOS and SMAP soil moisture retrieval algorithms, Remote Sensing of Environment, vol 192, pp 238-26, 2017

7. Mecklenburg S., M. Drusch, L. Kaleschke, N. Rodriguez-Fernandez, N. Reul, Y. Kerr, J. Font, M. Martin-Neira, R. Oliva, E. Daganzo-Eusebio, J.P. Grant, R. Sabia, G. Macelloni, K. Rautiainen, J. Fauste, P. de Rosnay, J. Muñoz-Sabater, N. Verhoest, H. Lievens, S. Delwart, R. Crapolicchio, A. de la Fuente, M. Kornber: ESA's Soil Moisture and Ocean Salinity mission: From science to operational applications, Remote Sensing of Environment, vol 180, pp 3-18, 2016

8. Louvet S. T. Pellarin, A. al Bitar, S. Galle, M. Grippa, C. Gruhier, Y. Kerr, T. Lebel, A. Mialon, E. Mougin, G. Quantin, P. Richaume, P. de Rosnay: SMOS soil moisture product evaluation over West-Africa from local to regional scale. Remote Sensing of Environment, 156, pp 383-394
9. Muñoz-Sabater, J.: Incorporation of microwave passive brightness temperatures in the ECMWF soil moisture analysis. Remote Sensing. 7(5), 5758-5784; 2015
10. Alyaari A., Wigneron J.-P., Ducharne A., Kerr Y., de Rosnay P., de Jeu R., Govind A., Albitar A., Albergel C. Muñoz-Sabater J., Richaume P., Mialon A.: Global scale evaluation of two satellite-based passive microwave soil moisture datasets (SMOS and AMSR-E) with respect to Land Data Assimilation System estimates, Remote Sensing of Environment, 149, pp 181-195, 2014
11. Muñoz-Sabater J., P. de Rosnay, C. Jiménez, L. Isaksen and C. Albergel: SMOS brightness temperatures angular noise: characterization, filtering and validation. IEEE Transactions on Geoscience and Remote Sensing, 52, (9), pp 5827-5839, 2014
12. Parrens M., J.-C. Calvet, P. de Rosnay and B. Decharme: Benchmarking of L-band soil microwave emission models, Remote Sensing of Environment, 140 pp 407-419, 2014
13. Albergel C., G. Balsamo, P. de Rosnay P., J. Muñoz-Sabater, and S. Boussetta: A bare ground evaporation revision in the ECMWF land-surface scheme: evaluation of its impact using ground soil moisture and satellite microwave data, Hydrol. Earth Syst. Sci., HESS, 16, 3607-3620, 2012
14. Albergel C., P. de Rosnay, C. Gruhier, J. Muñoz Sabater, S. Hasenauer, L. Isaksen, Y. Kerr and W. Wagner: Evaluation of remotely sensed and modelled soil moisture products using global ground-based in-situ observations, Remote Sensing of Environment, 118, pp215-226, 2012
15. Mialon, A., Wigneron J.-P., de Rosnay, P., Kerr, Y. and Escorihuela M.J.: Evaluating the L-MEB model from long term microwave measurements over a rough field, SMOSREX 2006, SMOS special issue of IEEE Trans. Geosci. Rem. Sens., 2012
16. Muñoz Sabater J.M., A. Fouilloux and P. de Rosnay, " Technical implementation of SMOS data in the ECMWF Integrated Forecasting System", Geosci. Remote Sens. Let., vol 9(2), 2012
17. Wigneron J.-P., M. Schwank, E. Lopez Baeza, Y. Kerr, N. Novello, C. Millan, C. Moisy, P. Richaume, A. Mialon, A. Al Bitar, F. Cabot, H. Lawrence, D. Guyon, J-C Calvet, J. P. Grant, T. Casal, P. de Rosnay, K. Saleh, A. Mahmoodi, S. Delwart, S. Mecklenburg: First evaluation of the SMOS and ELBARA-II observations in the Mediterranean region, Remote Sens. Env. 124, pp26-37, 2012
18. Muñoz Sabater J.M., P. de Rosnay, G. Balsamo, "Sensitivity of L-band microwave emission to soil roughness, Int. J. Remote Sensing, 2011
19. Wigneron J.-P., Chanzy A., Kerr Y., Lawrence H., Shi J.-C., Escorihuela M.J. Mironov V., Mialon A., Demontoux F., de Rosnay P. and Saleh-Contell K. Evaluating an improved parameterization of the soil emission in L-MEB, IEEE TGRS, vol 49(4), 1177-1189, 2011
20. Schwank M., I Völksch, J.-P. Wigneron, Y. Kerr, A. Mialon, P. de Rosnay, C. Mätzler, Comparison of two surface reflectivity models and validation with radiometer measurements, IEEE TGRS, vol 48, pp 325-337, 2010
21. de Rosnay P., M. Drusch, A. Boone, G. Balsamo, B. Decharme, P. Harris, Y. Kerr, T. Pellarin, J. Polcher and J.-P. Wigneron, The AMMA Land Surface Model Intercomparison Experiment coupled to the Community Microwave Emission Model: ALMIP-MEM, J. Geophys. Res., Vol 114, 2009
22. Drusch M., T. Holmes, P. de Rosnay and G. Balsamo, Comparing ERA-40 based L-band brightness temperatures with Skylab observations: a calibration/validation study using the Community Microwave Emission Model, Journal of Hydrometeorology, Vol 10, pp213-225, 2009
23. Escorihuela M.J., Y. Kerr, P. de Rosnay, K. Saleh, J.-P. Wigneron, J.-C. Calvet: Effect of dew on the radiometric signal over a grass field at L-Band, IEEE TGRS Letter, 6(1), pp67-71, 2009
24. Holmes T., M. Drusch, J.-P. Wigneron and R. de Jeu: A Global Simulation of Microwave Emission: Error Structures Based on Output From ECMWF's Operational Integrated Forecast System, IEEE TGRS, 46(3), pp 846-856, 2008
25. Wigneron J.-P., A. Chanzy, P. de Rosnay, C. Rüdiger, J.C. Calvet, Estimating the effective temperature at L-band as a function of soil properties", IEEE TGRS SMOS special issue, Vol 46(3), pp797-807, 2008